

Wearable Material Properties: Passive Wearable Microstructures as Adaptable Interfaces for the Physical Environment

Yuyu Lin
Human-Computer Interaction
Institute
Carnegie Mellon University
Pittsburgh, Pennsylvania, USA
yuyulin@andrew.cmu.edu

Hatice Gokcen Guner
Carnegie Mellon University
Pittsburgh, Pennsylvania, USA
hguner@andrew.cmu.edu

Jianzhe Gu
Human-Computer Interaction
Institute
Carnegie Mellon University
Pittsburgh, Pennsylvania, USA
jianzheg@andrew.cmu.edu

Sonia Prashant
Carnegie Mellon University
Pittsburgh, Pennsylvania, USA
sprashan@andrew.cmu.edu

Alexandra Ion
Human-Computer Interaction
Institute
Carnegie Mellon University
Pittsburgh, Pennsylvania, USA
alexandraion@cmu.edu

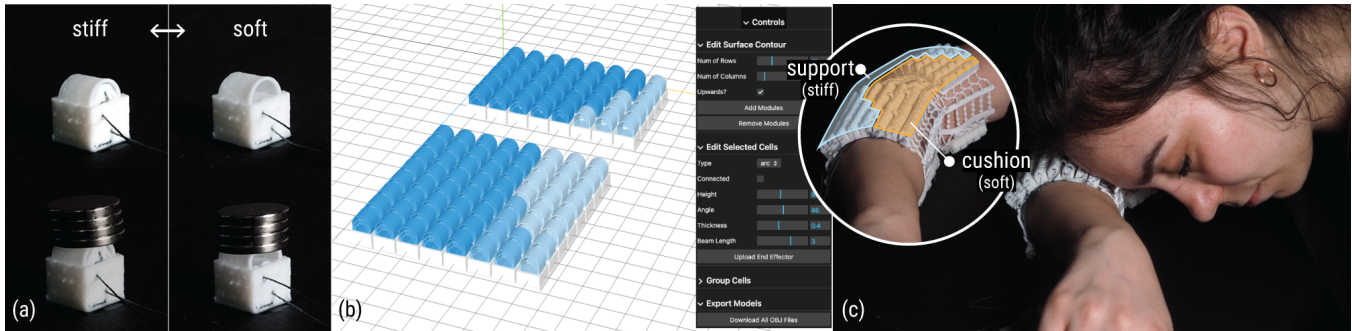


Figure 1: We present wearable material properties. They consist of (a) unit cells that can hold 2 discrete states to switch between 2 user-defined properties, including change in stiffness, height, shape, texture, or combinations of these. (b) We provide a design tool to assist users in defining their personal wearable material interfaces, such as (c) an arm-worn interface for cushioning on demand.

Abstract

Users interact with static objects daily, but their preferences and needs may vary. Making the objects dynamic or adaptable requires updating all objects. Instead, we propose a novel *wearable* interface that empowers users to adjust perceived material properties.

To explore such wearable interfaces, we design unit cell structures that can be tiled to create surfaces with switchable properties. Each unit can be switched between two states while worn, through an integrated bistable spring and tendon-driven trigger mechanism. Our switchable properties include stiffness, height, shape, texture, and their combinations. Our wearable material interfaces are passive, 3D printed, and personalizable. We present a design tool to support users in designing their customized wearable material properties. We demonstrate several example prototypes, e.g., a sleeve

allowing users to adapt to how different surfaces feel, a shoe sole for users walking on different ground conditions, a prototype supporting both pillow and protective helmet properties, or a collar that can be transformed into a neck pillow with variable support.

CCS Concepts

• **Human-centered computing** → **Human computer interaction (HCI)**.

Keywords

Wearables, Material properties, Digital fabrication, Metamaterials

ACM Reference Format:

Yuyu Lin, Hatice Gokcen Guner, Jianzhe Gu, Sonia Prashant, and Alexandra Ion. 2025. Wearable Material Properties: Passive Wearable Microstructures as Adaptable Interfaces for the Physical Environment. In *CHI Conference on Human Factors in Computing Systems (CHI '25)*, April 26–May 01, 2025, Yokohama, Japan. ACM, New York, NY, USA, 16 pages. <https://doi.org/10.1145/3706598.3714215>



This work is licensed under a Creative Commons Attribution 4.0 International License. *CHI '25, Yokohama, Japan*

© 2025 Copyright held by the owner/author(s).
ACM ISBN 979-8-4007-1394-1/25/04
<https://doi.org/10.1145/3706598.3714215>

1 Introduction

We interact with physical objects every day. We are familiar with how different materials *feel*, e.g., the firmness of a sofa, the rigidity of a desk, the softness of a pillow, etc. Most of these objects in our daily lives are static: their properties are baked in when they are being manufactured and they do not adapt to users after that. However, users might have different preferences for what is comfortable to them, or they might have different needs at different times for the same object, making *adaptable* physical objects and materials desirable.

Dynamically adapting how things feel to users has gained substantial interest, with researchers typically employing one of two approaches: either augmenting the physical objects themselves or augmenting users with wearable (haptic) feedback devices.

A variety of dynamic interfaces to replicate or *augment physical objects* have been explored in the past. Researchers have explored designing materials with complex microstructures [3, 41] to adapt object properties. Examples include fabricating items like shoes [3] or toys [41] with localized elasticity or pre-programming 3D shapes into flat prints for later activation [47]. Beyond static designs, one property of objects like seats [48] or door handles [16] can be manually configured. To achieve reversible and dynamic properties, adding actuation is often required. Implementations of such active systems include stationary desk-like shape displays that can imitate or manipulate existing materials [9, 34], or robotic constructs to explore dynamic walls [11] or floors [18, 44]. Since these interfaces augment the objects themselves, users don't always have access to them as they move between different spaces.

Wearable devices are a complementary approach since the interface is intended to stay with users. While many wearable devices designed for specific tasks in extended reality scenarios have been investigated (e.g., [8, 27, 43]), wearables that are intended to be worn during everyday tasks are rare. Examples include wearable actuators providing resistance and guidance [21], or shape-changing wearables for aesthetics [2, 49]. While these wearable devices are always available to users, they don't alter how everyday objects feel to users. The most closely related exploration of wearables allowing users to alter the interface between their bodies and their environment has been demonstrated as a shoe sole that can be changed from flat to corrugated and back [16], featuring only two different textures without the ability to alter other material properties.

In this paper, we investigate how to allow users to alter how their body interacts with objects that are typically under their control, e.g., how a chair in a conference room feels to them. To put users in control, we investigate this question by devising microstructures that support users to design custom multi-functional wearable interfaces that can be switched among various user-defined material properties and areas.

1.1 Passive Wearable Microstructures

To explore this concept, we introduce *wearable microstructures* which are passive structures that can be worn under clothes and can be switched to adapt to user needs. Our *design goals* are (1) to give users control over how their body interacts with other objects, (2) to allow them to tailor their interface to their need, (3) to integrate multiple functions and properties that they can choose to activate

while on the go while (4) keeping the interface small, easy to use and to maintain. We illustrate how we envision such wearable material interfaces to be used in Figure 2. A user is in a meeting and sitting on a rigid chair, but they wish to be more comfortable, like in a sofa chair. Typically, they would not be able to change the chair's material properties. We envision wearables designed to act as an interface between the user's body and the objects they interact with, here a chair. Users can control how the chair feels to them by controlling their own wearable interfaces. In the example in Figure 2b, they change their arm- and back-worn interface to make the rigid chair feel like a cushioning sofa chair. Additionally, they change their neck-worn interface to support their neck similar to a high-back office chair. After the meeting, the user takes a power nap in their office, for which they change their arm-worn interface to be partially soft cushioning their resting head and partially rigid to stabilize their head position (Figure 2c). After their workday is done, they switch their arm-worn interface to fully rigid to distribute the weight of shopping bag straps over their arm (Figure 2d).



Figure 2: We envision embedding the properties of (a) surrounding objects into (b) wearable devices to provide personalized, adjustable, and perceivable properties (c-d) at different locations.

To enable such interactions in line with our design goals, we design a wearable interface. Users can wear these material interfaces in order for them to be accessible when needed (addressing design goal 1), e.g., for cushioning during a spontaneous power nap, as depicted in Figure 1c. We designed our wearable interface to be modular such that users may customize it to their needs (e.g., tasks, environments, body-parts), as specified by design goal 2. Our wearable consists of many unit cells, shown in Figure 1a. Our unit cell embeds a bistable spring to switch between and hold one of

two stable positions without external energy. The two states can be designed to support the transition between different stiffnesses, heights, shapes, textures, or combinations of these. These discrete states can be designed by users, which we support with a web-based 3D editor shown in Figure 1b. Many cells can be combined and grouped to be configured together, as shown in Figure 1b-c. Tailoring the individual unit cell properties and their grouping allows users to integrate multiple reversible functions which they can activate as their needs change, addressing design goal 3. To keep the wearable interface small and easy to use (i.e., design goal 4), we choose to keep our wearable unpowered, as actuator can make interfaces bulky. We integrate a small tendon-driven switching mechanism to switch groups of cells between their designed properties. In our prototypes, users pull the tendons manually, however, our interface is agnostic to the actuation mechanism, which could be complemented by external actuation (e.g., motors), if needed. To the best of our knowledge, our interface offers the most functions within an unpowered and wearable form factor.

Contributions. Our main contribution lies in the *concept of making material properties wearable* and therefore always available for users. To instantiate this concept, we make the following specific contributions:

- (1) *Unit cells with discrete tunable properties.* We present small compliant structures that can be designed to employ two discrete user-defined property states, which they can switch between. When designing a unit cell, its properties can be chosen on a continuous scale (e.g., vary stiffness continuously). After fabrication, users can repeatedly switch between the two chosen discrete properties.
- (2) *Unpowered switching of custom material property patterns.* To enable users to switch groups of cells at once, we present a tendon-driven mechanism that can toggle the state of multiple cells.
- (3) *Design tool.* We build an interactive design tool that allows users to design custom wearable material properties.
- (4) *Application exploration.* We explore the utility of our wearable material interfaces through various application examples, including a convertible backrest/helmet, a combination of support collar and neck pillow, an arm-worn material interface, and a multi-functional shoe sole that can be repeatedly switched for wet, flat, or rocky ground conditions. The interactions we demonstrate are unpowered and integrated with users' context.

We note that our research prototypes do not center around usability. Smaller form factors or integration with textiles would be desirable in the future. The scope of this paper includes the initial exploration of switchable geometry and utility of this novel concept.

2 Related Work

Our work builds on previous work on shape-changing inferences that typically instrument the environment, on wearable interfaces that instrument the user, on interaction mechanisms for unpowered interfaces, and on findings in microstructures and their corresponding material properties.

2.1 Changing physical objects dynamically

Dynamic interfaces enable interactive environments to adapt to users' needs. A variety of such interfaces, spanning from shape-changing interfaces to programmable matter, have been explored in the past. Such interfaces are appealing because they can convey dynamic affordances [7, 22, 23] and change their shape to adapt to users' needs.

A variety of implementations have been investigated. They include stationary desk-like shape displays that can imitate or manipulate existing materials [9, 34], hand-sized programmable structures (e.g., [25, 33]), or large scale robotic constructs to explore dynamic walls [11] or floors [18, 44].

This subset of constructs is part of a larger body of work, all of which augment the environment to assist users' needs in situ. In our work, we are looking for interfaces that are available to users at all times they choose to, which means making them portable or wearable. We focus on wearable interfaces for better integration in users' daily lives.

2.2 Wearable interfaces

Wearable interfaces augment the user, rather than the environment, and are therefore available as users move between different spaces. Often, wearable devices have been developed to provide computer-controlled haptic feedback for extended reality (XR) scenarios such as providing variable mechanical resistance [5, 6, 8], alter the perception of weight [14, 27, 43], temperature [28], stiffness [1, 45], or tactile notifications encoded in pinching or stroking across users' skin [13]. Beyond haptic feedback for XR, haptic feedback has been shown to convey dynamic affordances to users for actions over time (e.g., shaking a spray paint can) [26].

Shape-changing wearable interfaces are parallel research stream of wearable dynamic interfaces. Moldable interfaces can conform to the users body after heating and shaping, after which they rigidify to offer support [12, 37]. Active interfaces have also been explored as part of clothing to, e.g., change the clothing's permeability [49], shape [2], add expressivity [32], or offer guidance through resistance [21].

In our paper, we develop wearable interfaces, but not for haptic feedback or shape-change, but for users to adjust how existing objects feel.

2.3 Unpowered interaction

While actuated interfaces offer many functions and flexibility that can be computer-controlled, they come at a higher complexity and maintenance need. On the other end of the spectrum, passive or unpowered interfaces typically offer less flexibility but are interesting because of their simplicity and low maintenance. Often, such unpowered systems are 'human-powered', where users trigger the system by deforming it as part of the desired interaction. Examples include mechanical computation systems that utilize user input to trigger their programs [17, 19, 29], systems that harvest and store user-generated energy [30, 46], or manually tendon-actuated systems (e.g., [2]). Some active material can be triggered through changes in the environment, such as humidity, temperature, or (UV) light exposure, typically in a slow timeframe (e.g., [49]).

We build on these benefits of low complexity and maintenance and use tendon-driven user-powered actuation in our wearable material interfaces.

2.4 Engineering material properties

Through the emergence of additive manufacturing, unprecedented opportunities for fabricating objects with high geometric complexity opened up. As designed or architected microstructured material can exhibit unprecedented characteristic, such as abilities to expand in volume ('auxetics', e.g. [39]) or absorb shocks (e.g., [42]). 3D printed engineered structures can emulate existing composite materials [3], give objects localized elasticity [36, 41] and haptic force feedback [50], or implement mechanical [15], kinetic [35] and decision-making capabilities [17, 19].

While many such 'metamaterials' are defined before fabrication, new work covers how to reconfigure them after fabrication. Typically, a mechanism that allows the material the change their shape is integrated into the structures, e.g., as flexures [16], hooks [48], bistable structures [51], or through magnets activated by a stationary machine [4].

We build on the concepts from compliant mechanisms and metamaterials for our unit cell design with bistable structures. While we base our design on the general design of bistable structures, we design a novel unit cell with multiple user-defined and adaptable properties, including height, shape, texture and stiffness change.

3 Adaptable properties through unit cells

To design a wearable interface in a small form factor that can employ several functions for users to switch to based on their needs, we propose passive unit cells that can be assembled into conformable wearables. As our basic building block, we propose a unit cell that can switch between two distinct states passively. As we show in Figure 3, our cell consists of two main components: (1) the bistable switch and (2) the end effector.

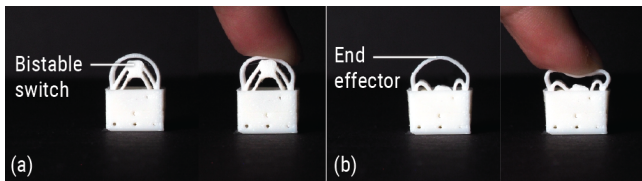


Figure 3: Our cell is designed to hold two discrete states. It embeds a *bistable switch*, which (a) when "on" (i.e. extended) can provide stiffness to the cell yet (b) when "off" (i.e., collapsed) allows the *end effector* to govern the material properties.

The *bistable switch* is a bistable spring that is embedded inside the cell and allows users to switch between the cells' states. When the bistable switch is "on", i.e., when the spring is extended, the material properties are mainly governed by the properties of the spring, which dictates the stiffness of the cell. To switch the material into its second state, we push the bistable spring down to snap-through into its collapsed state, which allows the *end effector* to govern the cells' properties. Bistable structures have been frequently used in the past to reversibly configure materials without the need for

actuation [4, 17, 19]. We print the cells using consumer-grade fused-deposition modeling 3D printers and off-the-shelf flexible filament (Ninjaflex, TPU 85A) with an outside side length of 9.2 mm.

3.1 Designing the "on" state

In this state, the properties of the bistable spring govern the major mechanical properties of the cell, as shown in Figure 4a. The bistable spring can be designed to control how stiff the cell is overall (which is often referred to as "programming" or "tuning" the material (e.g., [10, 24, 40]). Figure 4a illustrates 3 examples of bistable springs varying in stiffness, and 3 other examples varying in both stiffness and height. We characterize the stiffness and geometric parameters for a variety of bistable springs in Section 6. By introducing a gap between the bistable spring and the end effector (see Figure 4c), we can design the non-linear stiffness profile of the "on" state. That gap causes the end effector properties to be dominant at first before the cell is displaced enough to contact the bistable spring, at which point the bistable properties govern the properties.

3.2 Designing the "off" state

In the "off" state, the bistable spring is depressed until it snaps through into its second stable position, which is collapsed. With the bistable spring out of the way, the end effector is left to govern the material properties of the cell. While the cell's geometry (i.e., its overall shape) defines its properties, we break it up into four dimensions to aid design. In Figure 4b, we illustrate four main characteristics that our end effector controls: stiffness, height, shape, and texture. Additionally, the connection structures between the bistable switch and end effector can change end effector geometries and thus material properties in the "off" state. When connected (Figure 4c), end effector deforms with collapsed bistable switch, which can change the cell height, shape, or hide or reveal textures.

3.3 Unit cell properties

Material properties are very broad and include, e.g., vapor permeability, thermal conductivity, color, transparency, porosity, etc. In this paper, we focus on a subset of mechanical properties, i.e., stiffness, height, shape, and texture (as Figure 4c shows). These properties will allow users to configure their interface to adapt to different needs in elasticity, friction, damping, shape, or tactile features.

Stiffness. Stiffness is a core material property that defines how hard a material feels. Materials with switchable stiffness can be adjusted to a soft state to make rigid materials and surfaces feel softer, or configured to a stiffer state to distribute load. We demonstrate this property by an arm sleeve and back cushion applications in Section 5. The "on" state stiffness is mainly determined by the bistable spring. The "off" state stiffness can be tuned by the thickness of the end effector.

Height. Height defines the order in which the cells are physically felt, with taller cells being perceived first. For example, in our neck interface application we present later, users can adjust the height of support in different regions of the neck. The end effector can vary the cell's overall height, which can be designed to be dependent or independent of the bistable switch. By adding a small connection

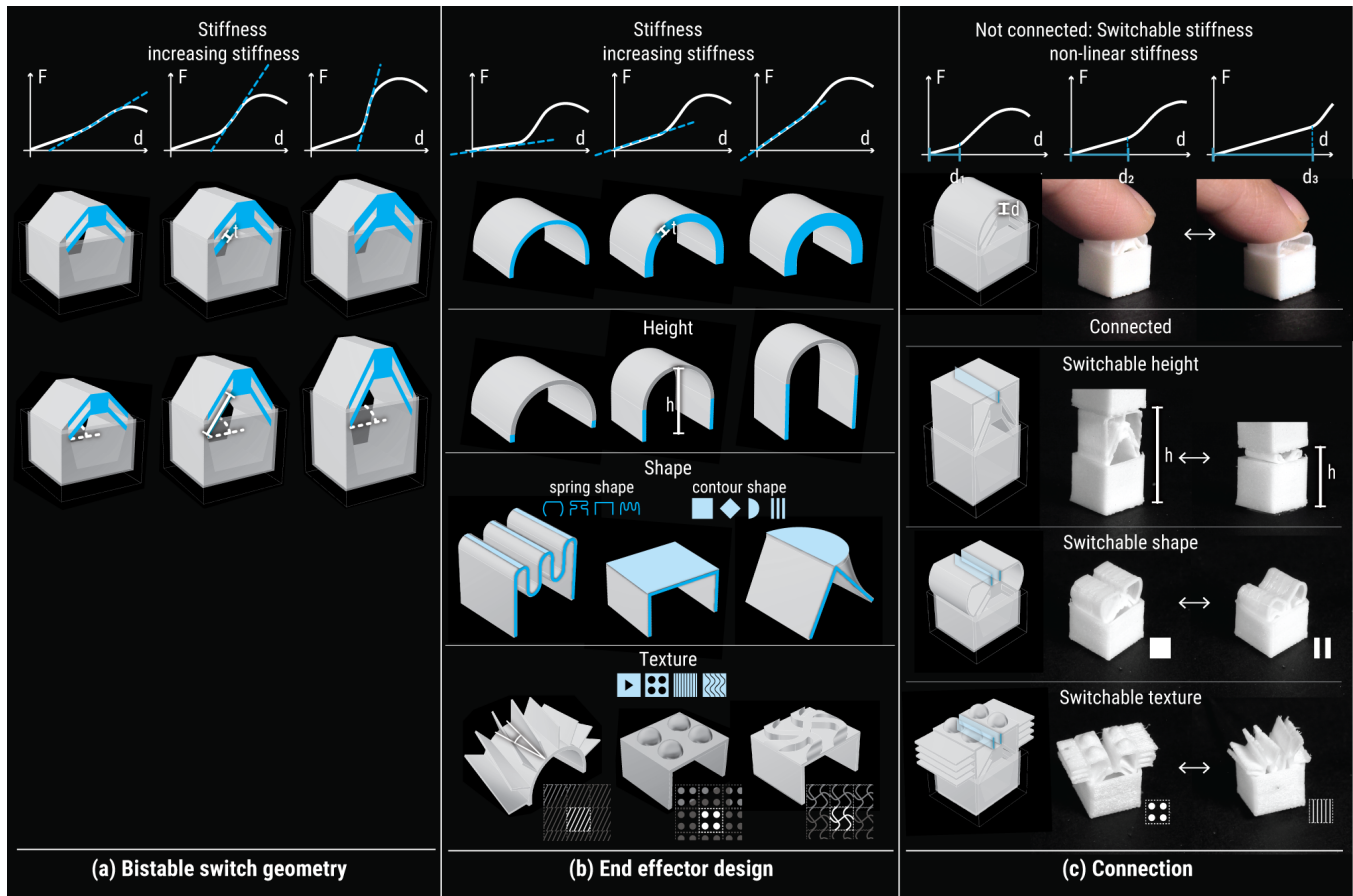


Figure 4: The switchable material properties in a unit cell are defined through the combination of three key components: (a) bistable switch geometry, (b) end effector design, and (c) whether they are connected.

between the structures, the cell can be designed to change its height, i.e., to shorten when switched from the "on" to the "off" state. By omitting a connection, the end effector maintains its height after state switching. As mentioned, the bistable spring can be adapted in height to create linear or non-linear stiffness in the "on" state.

Shape. Shape is the overall 3D form and profile of the cell, which affects the external contour of each unit. For example, we design rounded cells to accommodate loads from varied directions, such as supporting the head while napping in our arm sleeve application. Meanwhile, rectangular contours are applied on a shoe sole to ensure stability, where loads mostly come from a single direction. The shape of the end effector can be designed freely and independently from the bistable spring. Additionally, by connecting the end effector and bistable switch structures, cells can be configured to employ shape-change after switching the cell's state. For example, we illustrate in Figure 4c how to embed flexures to control the cell changing from a straight top to a rounded surface.

Texture. The macro-scopic texture within the contour shape determines the tactile sensations, including variations in patterns and orientation. For example, it can be designed to alter friction or create channels for water as we will present in the shoe sole

example. Again, we can embed texture-change, e.g., by applying textures to the side of the cell's end effector, which are inaccessible to users, that fold up after the cell's state has been switched. This exposes the previously hidden textures to the reachable surface.

3.4 Combining cells into surfaces

Users can combine material properties into wearable sheets to design their personal material interfaces. In Figure 5, we show 4 examples of such material interfaces as an initial inspiration. The unit cells of a wearable material can be switched individually or in a group. If each cell is switched individually, a material with n units can have 2^n possible variations. In Figure 5, we demonstrate different switching methods in a group: separately, together, or sequentially. With more types of cells and grouping layouts, many more combinations and switching modes are possible, further expanding the design space for customizable wearable material properties.

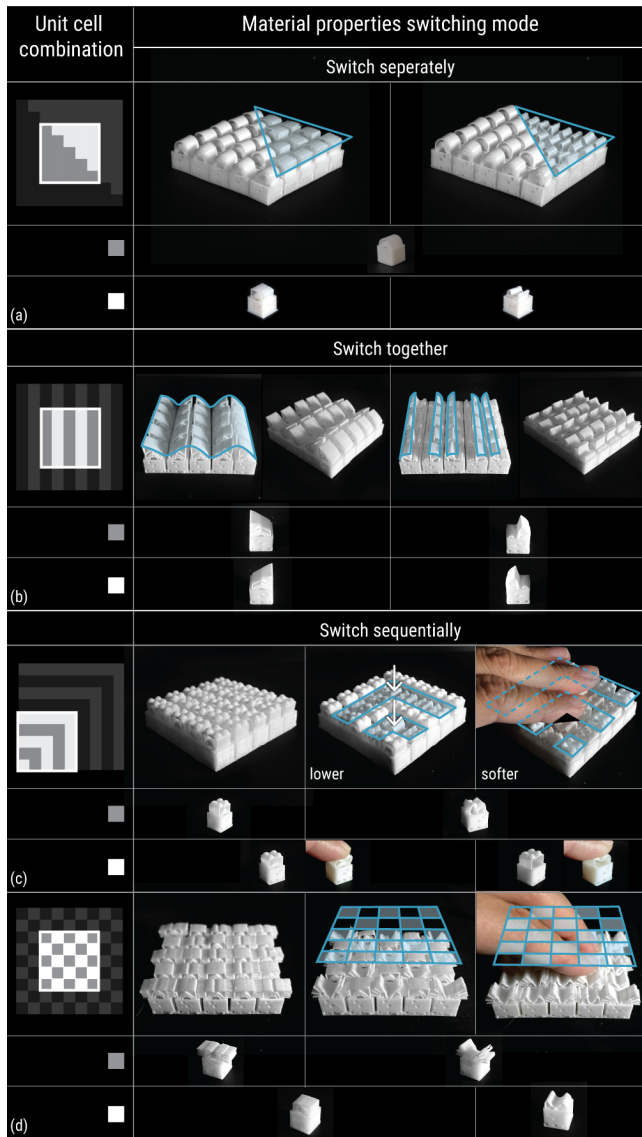


Figure 5: We illustrate four of many possible ways to combine two types of cells with switchable material properties, e.g., in (a) diagonal, (b) striped, (c) radial, or (d) checkerboard layouts. With different switching sequences, these combinations demonstrate diverse functionalities: (a) Changing the shape and height of one type of cell. (b) Altering the shape of all cells together from rounded to spiked shapes. (c) From a planar dotted texture surface, we first adjust the height of the cells to create a radial pattern. Subsequently, we switch the stiffness of the remaining cells so that the radial pattern is felt first, followed by the lowered cells. (d) From a flat surface, the hair texture is revealed on half of the cells, while the rest transition to grooves as their shapes change.

4 Switching many cells

While the bistable switch could be pushed through to its second state manually, this would require users to switch tens (or potentially hundreds) of cells individually. To allow users to configure many cells at once, we present a tendon-driven actuation mechanism.

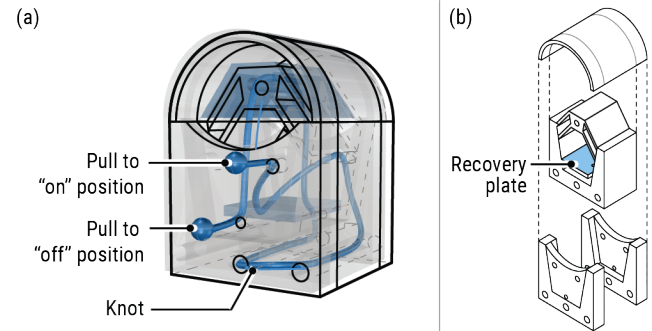


Figure 6: (a) Our tendon-based actuation uses a single tendon and can be pulled by its two ends, where one end can pull the bistable switch down and the other can lift our recovery plate, highlighted in (b), to push the spring back out.

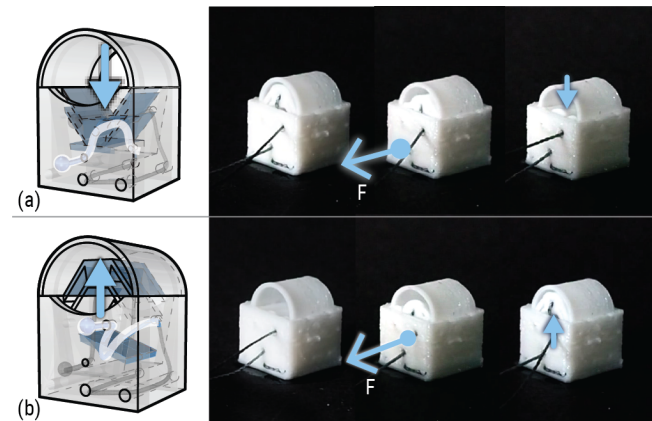


Figure 7: We illustrate how pulling the string actuates the embedded bistable switch (a) from "on" to "off" position and (b) from "off" to "on" position.

4.1 Trigger mechanism

We illustrate our tendon-based actuation in Figure 6. Our mechanism is designed to pull the bistable switch down into its "off" position and up into its "on" position with one single tendon. We keep it to one tendon by feeding it twice at a 90° angle through the front of the cell's walls. The friction resulting from redirecting the tendon holds it in place while allowing the two ends to trigger the deformation of the structural components. This eliminates the need to tie knots, which would be very tedious for hundreds of cells.

To trigger the bistable spring to switch into its "off" position, we feed the tendon through the walls of the cell and the top of

the bistable switch. As illustrated in Figure 7, pulling the tendon forward causes it to straighten out and pull the bistable switch down. To reset the cell back into its “on” state, we feed the tendon behind the knot mechanism through a recovery plate. As we show in Figure 6, when the tendon is pulled, it straightens which pulls the recovery plate up, which in turn pushes the bistable switch up.

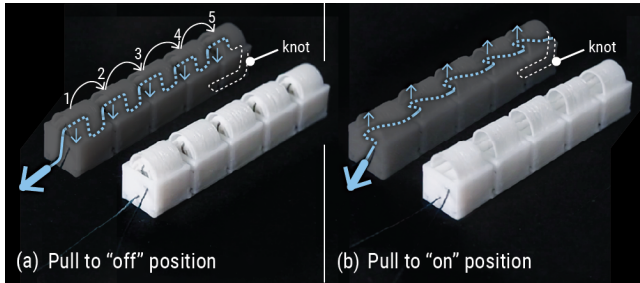


Figure 8: Switching the cells in a row with a single tendon. (a) One end of the thread can pull all the cells in a row to “off” position one by one; With the same knot mechanism in between, (b) the other end of the thread can pull all the cells in a row to “on” position.

4.2 Configuring surfaces

To allow users to configure and repeatedly change the state of their wearable material interface, we show how to combine the trigger mechanisms into multiple programmable patterns. For a simple illustration, we show connecting a row of cells in Figure 8. We keep it simple and make use of the flexibility of the tendons to route them under neighboring cells. We bundle them into a thread that users can then interact with.

Larger surfaces can now be designed to have integrated material programs, i.e., actuation patterns that are defined through how the individual trigger mechanisms are bundled. As shown in Figure 9, we can divide the surface into groups and adjust the overall stiffness by controlling the state of each group. More properties combinations can be achieved this way, such as switching texture, height, or shape. In each row, tendon can skip some cells so that only the cells that are connected will be switchable. By grouping these rows, we can achieve more precise control patterns, such as the patterns shown in Figure 5.

5 Application examples

We present several application examples illustrating how our body-worn material interfaces can be worn under or as part of clothing. We showcase how users can benefit from adaptation options that are always available to them.

5.1 Arm-worn interface

This example demonstrates an arm-worn interface composed of cells with a rounded shape and switchable stiffness, as the cell shown in Figure 3. After a long-haul flight, a user arrives for a meeting with their heavy travel bag. They wear the arm-worn interface in a stiff state to distribute the load of the thin straps over

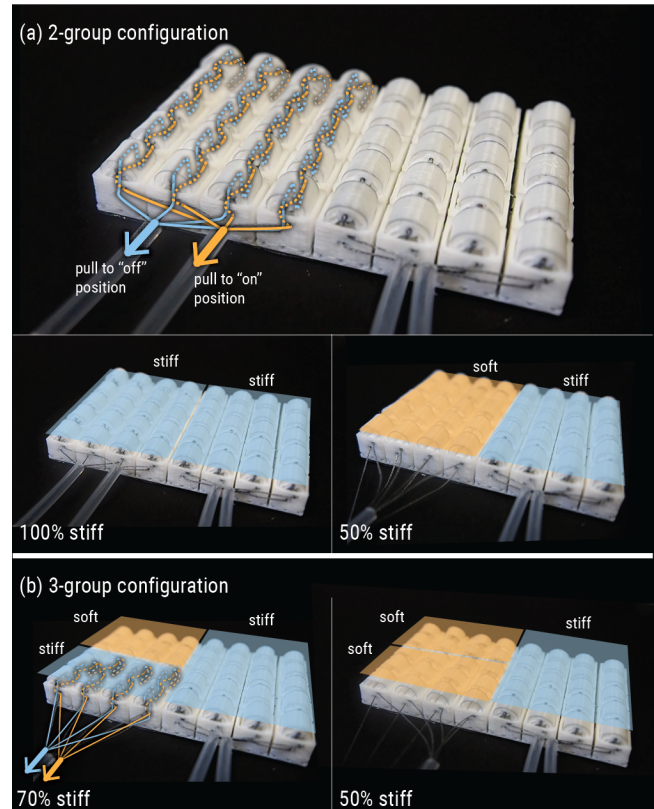


Figure 9: Switching the cells in a surface with grouped tendons, with the same actuation mechanisms in each row. (a) In a two-group configuration, four rows are combined as a group. This configuration has three states: 100% stiff, 50% stiff, and soft. After switching one group to the “off” position, the stiffness of whole surface reduces from 100% to 50% stiff. (b) In a three-group configuration with 8, 12, and 20 cells in each group. There are more states of stiffness: 100%, 80%, 70%, 50%, 30%, 20% stiff and soft. Note that the percentage represents the proportion of stiff cells on the surface.

their arm, as we show in Figure 10a. They sit at the conference table and find the chair’s armrest too hard. While they cannot change the properties of the armrest, they can change how it feels to them. To do so, they utilize their arm-worn material interface that they wear under their clothing, as we show in Figure 10b. The interface is configured into three groups to provide switchable support and cushioning for selective regions: two groups on the upper surface of the arm and one group on the underside. They transform the grouped cells on the underside to switch to their soft state by pulling the tendons that attach to their sleeve, for a more cushioned armrest (Figure 10c). As their co-worker leaves and the user is tired (Figure 10d), they switch the material on their upper and lower arm to act as a pillow for them to take a quick power nap. The wearable switches a part to soft for cushioning while the other parts are set to stiff to stabilize both their head and arm.



Figure 10: Our arm-worn material interface (a) can provide a protection padding when holding a bag during traveling, and (b) allow users to adjust the stiffness to adapt to the chair in shared spaces, (c) to have a more cushioned arm-rest. Users can use the upper part as (d) a selective-support cushion for a power nap.

5.2 Multifunctional shoe sole

Footwear selection significantly influences walking stability and safety across various terrains like uneven, wet, and regular level surfaces [31, 38]. In this application example, we demonstrate a shoe outsole with switchable properties to adapt to different conditions on the walking surface. The outsole is designed using three types of unit cells, as Figure 11 illustrates: stiffness-switchable cells

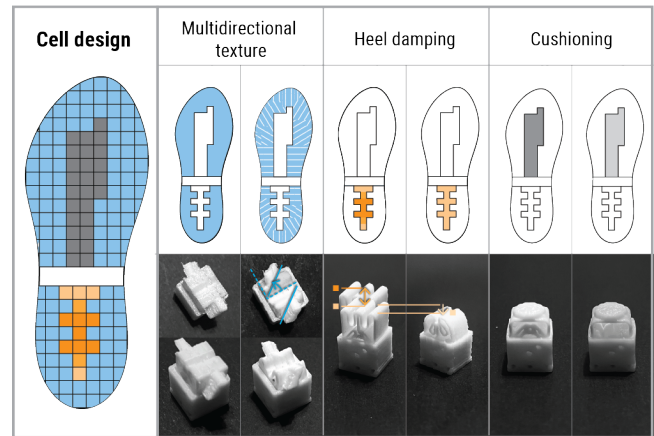


Figure 11: Our shoe outsole design is composed of three distinct types of cells, each specializing in switching multidirectional textures, height, or stiffness, respectively.

with button-textured end effectors, height-switchable cells with compliant spring end effectors, and texture-revealing cells that can expose textures in designated orientations. The combination of these cells is designed to improve comfort and safety when walking on flat sidewalks, wet or muddy paths, and uneven rocky surfaces. To switch the shoe properties based on the surface conditions, the tendons are grouped as shoe laces such that the user can pull on the corresponding laces.

For flat terrain like sidewalks (Figure 12a), the height switchable cells are in the high state, supporting progressive damping through a rounded, higher heel and a compliant spring shape. Note that the combined strength of all cells can support the user’s weight (55 kg in this example) without unintended actuation despite cells’ small form factor. During walking, the cells remain stable in their state without unintentionally switching. When walking in a wet and muddy area (Figure 12b-c), the texture-switchable cells in the outer regions of the outsole can be changed to reveal multidirectional grooves to drain the water and improve grip. The heel height is lowered to have a flat and level landing plane, for better walking stability. When walking on a rocky path (Figure 12d-e), sharp and irregular rocks can cause discomfort under the feet. In this case, multidirectional grooves are no longer needed, but the stiffness switchable cells in the middle area are switched to their soft states as protective cushioning to mitigate the impact of rough surfaces.

5.3 Back-worn interface

We demonstrate a larger multipurpose material interface that is worn on the back and is integrated with user’s clothing, as shown in Figure 13a. Here, a user carries a backpack and visits their friend. The backpack contains many small items and poor padding, which is uncomfortable. Therefore, they use the wearable interface entirely in its stiff state to distribute the pressure points and protect their back (Figure 13b). The user and their friend go for a walk. As they sit down and lean against a park table, the rigid edge bothers the user. They promptly pull the tendons to switch the material interface on their upper back (Figure 13c) into a softer property to make the



Figure 12: Our shoe outsole properties can adapt to (a) flat, (c) wet and (e) uneven surfaces. Users can switch the sole properties by (b,d) pulling the shoe laces.

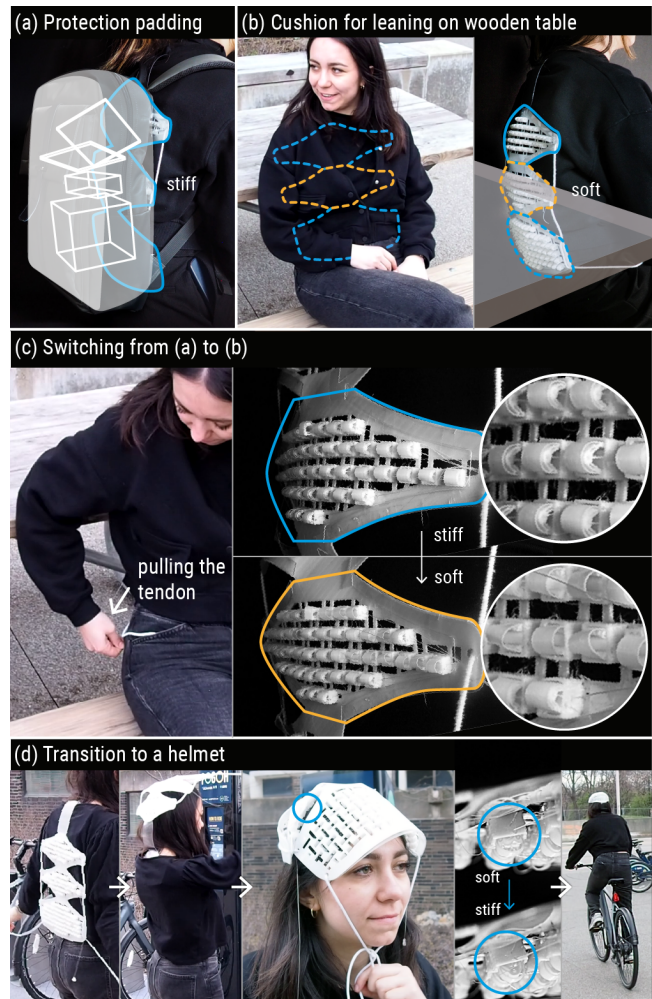


Figure 13: Our back-worn interface can provide (a) backpack padding or (b) adaptable cushioning against rigid materials like wood in shared space, through its (c) switchable stiffness properties. (d) It can also be transformed into an always-available bike helmet.

park table feel softer. As they decide to take a spontaneous bike ride, as illustrated in Figure 13d, they transform their wearable material into an impromptu helmet that can absorb and distribute the force of impacts between head and ground in case of an accident. We note that the helmet is a research prototype and did not undergo safety evaluations; however, we use this example to demonstrate the potential for such always-available adaptable material interfaces.

5.4 Transformable neck support

In Figure 14, we show a collar that consists of multiple cells with adaptable properties. We implement the stiffness- and height-changing cells column-wise (Figure 14a). For each column, the two bottom layers are integrated with our height-changing cells and bundled



Figure 14: (a) Our collar is designed with columns arranged around the neck, each column consisting of three types of cells. (b) The collar can be transformed into a neck support when the user feels strain in the neck. (c) Users can adjust the height to fine-tune their neck posture. (d) Additionally, users can modify the local stiffness for comfort.

together to adjust the column height, allowing users to tune the preferred height. The rest of the cells in a column are stiffness-changing cells, which allow users to adapt the local softness.

In this example, the user feels strain in their neck as they read a book (Figure 14b). To maintain proper posture and reduce strain, they need a neck support provided by an ergonomic chair with adjustable headrests. Now they embedded these properties into

portable and transformable wearable materials. They transform their collar into a neck support using the integrated drawstring (Figure 14c). They also adjust the stiffness when they want to lean to the side to rest, as shown in Figure 14d. This application example highlights how our wearable material properties can be integrated with other shape-changing structures for synergetic effects.

6 Technical Evaluation

We characterize the geometry parameters and their effect on the cell stiffness in this mechanical characterization study. We focus on evaluating the stiffness only as it is the most complex property to vary and core to our contribution. We first characterize single cells before evaluating how multiple cells together affect a surface's overall stiffness. We then characterize the forces required for the tendon-driven mechanism of cells with varied stiffness.

6.1 Experimental characterization of single cells

We first characterize the properties of a single cell. We measure the bistable switch and the end effector separately as these can be defined independently from each other. The full cell in its "on" state is characterized by the combination of the bistable switch's and the end effector stiffness. In the "off" state only the end effector stiffness takes effect.

6.1.1 Bistable switch stiffness. To understand the correlation between the stiffness properties and the geometry parameters of the bistable switch, we 3D printed 15 models with parameters varying in beam angle and length, as Figure 15 illustrates.

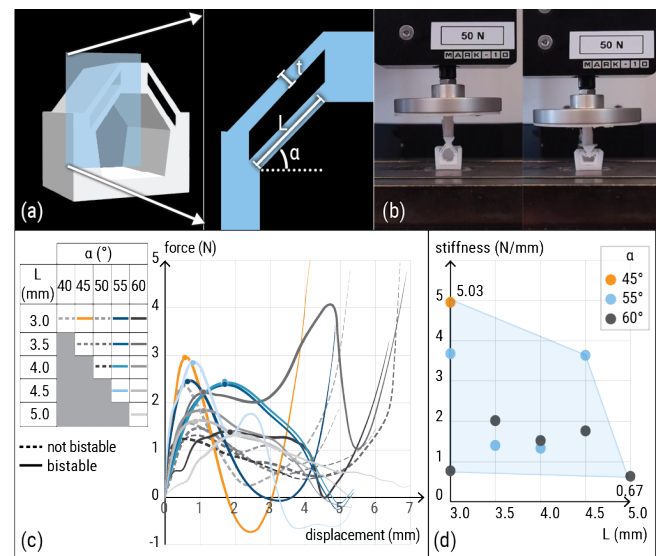


Figure 15: (a) Representation of thickness, length, and angles on the bistable switch geometry. (b) Setup on Mark-10 ESM 303 with a 50N force gauge. (c) The measurement results as force-displacement graphs. (d) Stiffness results with geometrical parameters of the 10 bistable cells.

We based our experiment design on [42, 51], who evaluated how the beam angle and the ratio of beam thickness and length

influence the bistable behaviors. Specifically, we vary the angle α between 45° and 60° in 5° increments, vary the length L of each beam of our bistable switch, and keep the thickness t the same (0.375 mm). All combinations would result in 25 samples, but 10 that are marked in Figure 15c in grey are infeasible as they result in interfering geometry, leaving us with our 15 samples. As we show in Figure 15b, we perform compression tests using a 50N force gauge (resolution of 0.02N) on our motorized test stand (Mark-10 ESM 303) and record force-displacement data.

Figure 15c shows the raw results of force over displacement. The dashed lines indicate non-bistable cells and solid lines bistable cells. The graphs show how during compression (displacement), the resisting force increases, reaches a peak force, and generally decreases when the spring switches state. We found that 10 of the 15 cells we sampled in this experiment are bistable and therefore suitable parameters for our stiffness-changing properties.

We summarize the effect of parameters on stiffness in Figure 15d, where we plot the stiffness calculated as the first local maximum force divided by the displacement (cf. secant modulus¹). We label the peaks used for this stiffness calculation with dots in Figure 15c. Our results in Figure 15d show that the angle and length parameters allows designers to define the behavior of the cells, with stiffness ranging from 0.67 to 5.03N/mm.

6.1.2 End effector stiffness. This short experiment is intended as a comparison to the effects of the bistable switch. We printed 6 cells with only arc-shaped end effectors. We varied the arc thickness from 0.2 to 1.2 mm and measured their stiffness using the same apparatus. We show the force-displacement graphs in Figure 16a, which are close to linear, as expected. We calculate the stiffness at 4 mm displacement, which is the distance between the arc-shape and the critical point during the switching process of the bistable switch. As shown in Figure 16b, our brief experiment confirms that the stiffness grows cubed with the thickness. This defines the "off" state of our cells. The "on" state is compound of the stiffness of the end effector and the stiffness of the bistable switch that designers choose.

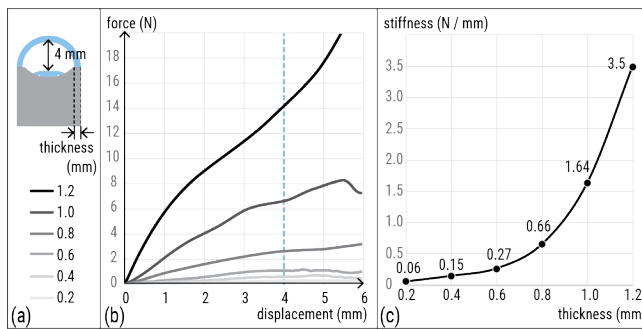


Figure 16: We measure (a) 6 arc-shaped end effectors and confirm that they (b) show linear stiffness in our force-displacement measurements and (c) that stiffness grows cubed with thickness.

6.2 Experimental characterization of surfaces

Since our wearable material properties are designed to be used as surfaces, we evaluated the change in stiffness with growing numbers of cells. As shown in Figure 17, we use a simple 3×3 surface and perform compression tests using the same setup as for the aforementioned single cell characterization. We measure the stiffness of the surface starting with all bistable switches "off" and cumulatively switching them into their "on" position one by one. We use 9 identical cells with beams of 0.6 mm thickness, 3.6 mm length and 58° angle. We had empirically determined these parameters to be reliable and expanded the aforementioned experiments based on them.

We show results in Figure 17c as the raw force-displacement graphs. The graphs show how the curves start out flat, which is due to the gap between the end effector and the bistable switch. Once the end effector contacts the bistable switch, the slope of force over displacement increases, i.e., the stiffness increases. This slope is maintained until the bistable switches snap into their off state, where the force-displacement graph flattens out. Overall, our measurements confirm that designers can modulate the stiffness of a surface by combining cell states appropriately. Surfaces with more cells in the "on" state exhibit greater stiffness. We acknowledge that these engineering metrics may not fully capture how humans perceive surface stiffness, such as for uneven configurations with mixed "on" and "off" states. Future work could use haptic discrimination methods [20], to assess how mechanical properties and cell sizes relate to perceived stiffness.

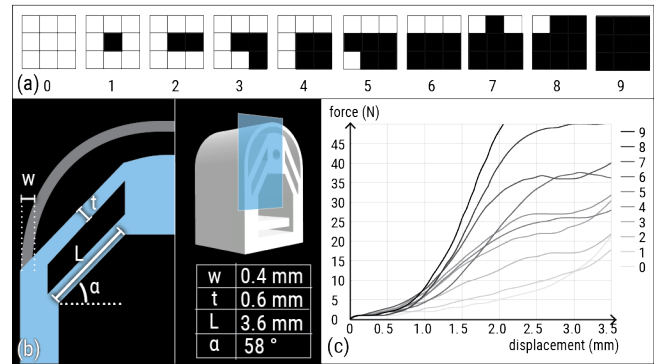


Figure 17: (a) We tested 10 configurations of a 3×3 surface with different numbers of cells in the "on" state. (b) The cells have the same geometry. (c) The force-displacement data from the compression tests.

6.3 Tendon-driven actuation

Since our passive actuation method is based on user's manual force, we further evaluated the force required for our tendon-driven actuation in relation to different cell stiffness. Specifically, we measured the pulling force needed to switch a single cell and a row of 8 cells (Figure 18a) with three different bistable switch geometries each. We select the bistable switches from our previous characterization in Figure 15: the stiffest ($L=3.0$ mm, $\alpha=45^\circ$), the softest ($L=5.0$ mm,

¹<https://www.instron.com/en/resources/glossary/secant-modulus-of-elasticity>

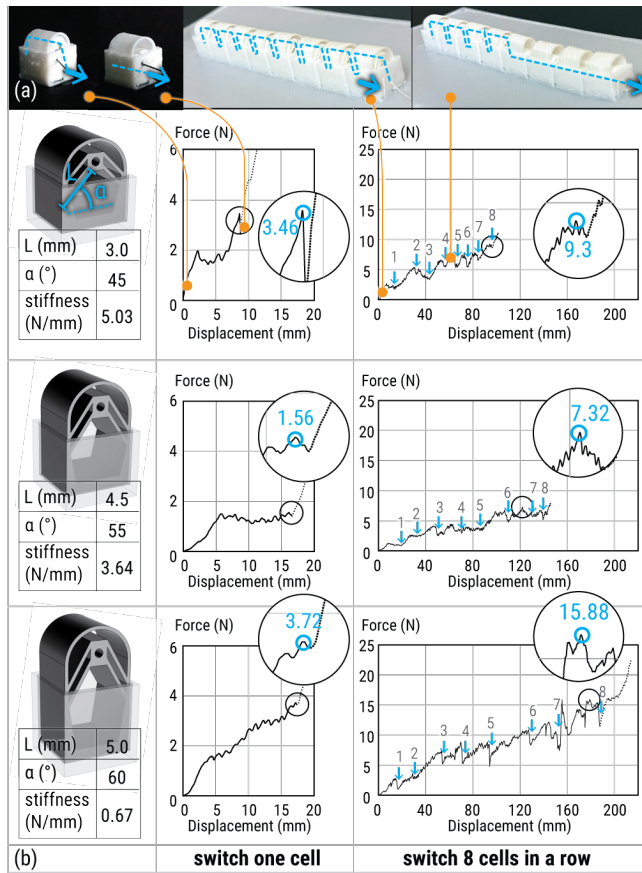


Figure 18: We measured the tendon pulling force of switching 3 groups of (a) single cells and 8-cell rows from "on" to "off" state. (b) The cells have different beam length (L), angle (α), and stiffness (left column). The middle column shows the force-displacement curves for switching single cells. The right column presents the force-displacement curves for switching 8 cells in a row, where we marked the position when each cell in a row successfully switched. The circled area in each curve highlights the maximum forces for switching.

$\alpha=60^\circ$), and an intermediate one ($L=4.5$ mm, $\alpha=55^\circ$). All end effectors were 0.4 mm arc shapes, with a consistent 1.2 mm distance between the end effector and bistable switch.

We installed the test patches in alignment with the movement direction of our Mark-10 test stand and recorded the force-displacement curves using the force gauge described above. For each measurement, the Mark-10 test stand pulled the tendon until we observed that the cell(s) all switched to the "off" state. Then the tendon was released to ensure that all cells remained stably in the "off" state without external force.

The resulting force-displacement curves are shown in Figure 18b. The left column shows the force required to *switch a single cell* using our tendon mechanism. The required force for each patch is the maximum force by the last increase—after successfully switching

each cell, the force decreases while the tendon continues to pull on the knot (seen in the graph where the force increases drastically at the end). Our results show that switching a single cell into its "off" position using our tendon takes less force than pushing the bistable spring down for the first two cells. The tendon-driven switching force for the first cell is 3.46N compared to the cell stiffness of 5.03N from our previous evaluation. For the second cell, we measure 1.56N using the tendon compared to 3.64N. Interestingly, the third cell requires 3.72N of pull force on the tendon for a cell with only 0.67N of stiffness. This may be due to the long path of switching such a tall cell creating friction on the tendon. More data may help understand this phenomenon further. We note that we did not use such tall bistable springs in our application examples yet included it in our evaluations to investigate the boundaries of our geometry parameters.

The results of switching a row of 8 cells are shown in the right column of Figure 18. Since our tendon mechanism is designed to switch the cells sequentially when pulling, the force required to switch a row of cells is not linearly proportional to the number of cells. We label each cell switching on the local minima in the force-displacement graphs, which we verified with our recorded videos. For example, for the bottom two cells in Figure 18b, the force of switching the 5th cell is lower than that of switching the 4th. This is because, after a cell switches to the "off" state, the tendon in straightens out potentially causing a reduction in friction. We may further minimize the friction by fine-tuning the alignment of the holes in the collapsed bistable switch and the cell frame, to keep the tendon as straight as possible. We acknowledge that while the row-wise switching does not linearly sum forces, pulling multiple rows in parallel would.

7 Design tool

To support users in designing their preferred wearable material properties, we present a web-based design tool² (Figure 19) that allows users to create compliant unit cell structures and export them for 3D printing. The tool provides an intuitive and accessible interface for users to define the structure contour, edit cell type and parameters, visualize their designs, and export for 3D printing.

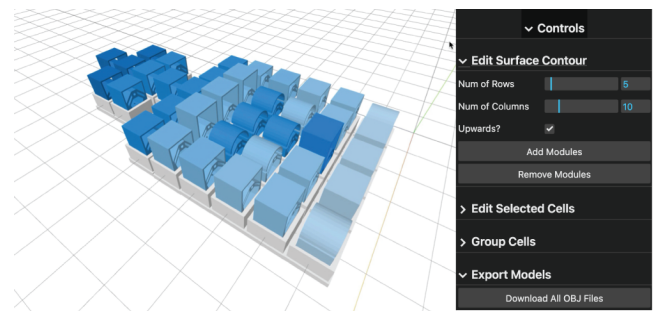


Figure 19: Web-based editor. Left: 3D viewer of the designed structure. Right: Options and tools for global and selected units parameters.

²<https://interactive-structures.org/wearable-mat-prop/>

7.1 Contour editing

Users can define the contour of their structure using two methods. The first method allows users to enter the number of rows and columns to create a rectangular contour (Figure 20a). Alternatively, users can use the selection tool by clicking and dragging the mouse to draw a square selection box, or by pressing "shift" to append cell selections. Users can then click "add modules" or "remove modules" to create organic shapes (Figure 20b). Additionally, users can check the "Upward?" option to orient all units in either a laying down or standing up position (Figure 20c).

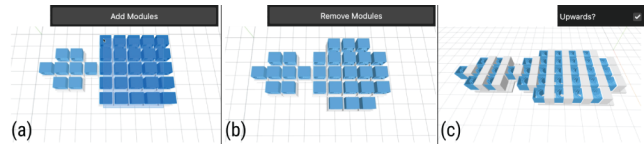


Figure 20: Editing the contour. (a) Brushing an area and add modules. (b) Selecting multiple modules and delete them. (c) Changing the orientation of all the modules.

7.2 End effector editing

Using the 8×5 patch in Figure 21a as an example, users can edit the type of end effector for each cell. The default end effector is set to "flat". Users can select a cell and change the end effector to "arc" for arc-shaped end effectors, "ori" for origami-shaped end effectors, or "cus" to upload a personalized CAD model for customized end effectors (Figure 21b).

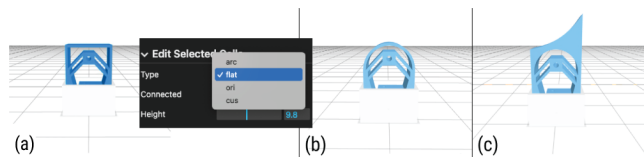


Figure 21: Editing the end effector. (a) Original cell. (b) Change the end effector from square to arc shape. (c) Upload a customized model as end effector.

7.3 Stiffness and Height Adjustment

After defining the end effector types, users can further specify the parameters for a single (Figure 22) or a group of cells (Figure 23) to adjust their stiffness and height. By selecting a group of cells (including those with different end effectors) and dragging the sliders, users can modify the total stiffness and height of all the selected cells. The color of the cells changes based on the stiffness, which is calculated using the "thickness" and "beam length" parameters.

7.4 Grouped tendon visualization

After designing the cell properties, users can configure the cells into groups (Figure 24a). The design tool can visualize how the tendons are routed through these groups, aiding in the assembly process (Figure 24b).

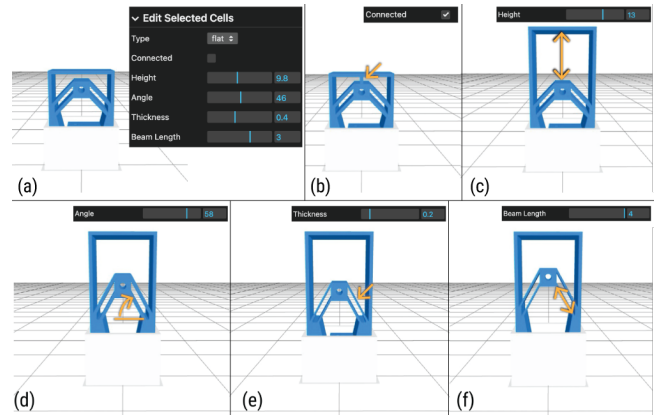


Figure 22: Editing the type and properties of the (a) a cell by (b) connecting the bistable switch to the end effector. (c-f) adjusting the height, angle, thickness, and beam length.

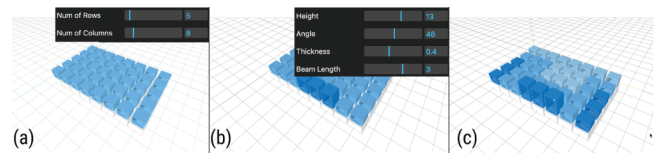


Figure 23: Editing a group of cells. (a) A 8×5 patch. (b) Changing the height of one row and the beam thickness of some cells. (c) The color shows the stiffness of the cells.

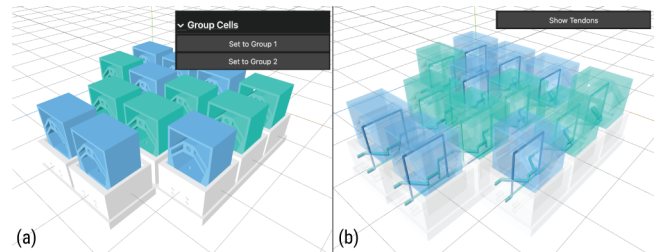


Figure 24: (a) Editing the grouping of cells. (b) Visualizing the tendons of each group.

7.5 Model Export

Once satisfied with their design, users can click the "Download All OBJ Files" button to export each cell model and the bottom model in OBJ format, which is ready for 3D printing.

7.6 Implementation

The design tool is implemented using Three.js³ for geometry visualization and interaction, lil.gui⁴ for the menu, and OpenJSCAD⁵ for geometry generation, modification, and download. The entire application runs on the client side, ensuring a seamless and accessible user experience.

³<https://github.com/mrdoob/three.js>

⁴<https://github.com/georgealways/lil-gui>

⁵<https://github.com/jscad/OpenJSCAD.org>

8 Discussion & limitations

Fabrication of our prototypes. The designs for our wearable material properties are entirely compliant, i.e. to be made in one piece without assembly. However, the research prototypes we presented in this paper were made by printing the core cell (bistable switch with the end effector as shown in Figure 3) separately from the array of boxes that holds them. We 3D print them separately because we use FDM printers with Ninjabflex filament, which is not feasible to print using overhangs or support material. We experimented with SLA printing, but found the need for internal supports infeasible. SLS printing will be able to print the entire prototypes in one piece, which users can access using professional 3D printing services (e.g., Shapeways, 3DHubs, etc.). Embedding the tendon for actuation is the last step after 3D printing, and it can be done either by the maker or by professional manufacturing.

Actuation. In this paper, we focused on developing passive structures that users can actuate themselves. Passive objects are beneficial since they require low maintenance, don't require batteries to be charged and overall consist of fewer parts. The passive nature of our interfaces comes at the cost that users need to preselect a small number of functions that they want to switch before fabrication. Additionally, inserting the tendon for actuation adds an assembly step. In the future, we plan to investigate the embedding of active materials (e.g. shape memory alloys, liquid crystal elastomers, etc.) into our structure to dynamically control the properties of the material.

Additional material properties. In the current scope of the paper, we focus mainly on mechanical properties such as stiffness, or texture change. In the future, we are interested in exploring thermal properties as well. We envision novel structures to change the permeability of clothing or printing with conductive materials to manage heat dissipation, etc.

Scale. Since our cell designs are fully compliant, they can be applied on different scales. Printing them in smaller scales would make for a superior wearable experience, while fabricating them in larger scales allows for more extreme ranges in material properties (e.g., stiffness). The achievable resistance to forces and the scale of the cells are correlated, i.e., larger scale cells can be made stiffer than smaller scale cells. We plan to experiment with different scales, materials, and geometries in the future.

Focus on wearables. Lastly, in this paper, we intentionally focused on exploring the concept of wearable material properties, due to their benefits of being always available to the users. However, we acknowledge that users can apply our materials on physical objects as well, if they wish to change their properties.

9 Conclusion

We presented the concept of wearable material properties. Adaptable physical interfaces and materials often require instrumenting the objects themselves, however users in shared space might not have control over how the objects feel or behave. In contrast, we investigated instrumenting the user. We presented a compliant, 3D-printable bistable switch allowing users to change the material

properties they interface with locally and across a surface. To illustrate how such wearable material interfaces can be useful, we implemented an interface worn on the arm and under clothing, worn on the back for comfort and protection, and worn as a collar for support. In the future, we believe that such wearable material properties can provide benefits in medical and rehabilitation uses, e.g., as self-adaptable orthotic devices.

Acknowledgments

This work was partially supported by the CMU Center for Machine Learning and Health (CMLH). We also thank Lea Albaugh for her help in proofreading.

References

- [1] Ahmed Al Maimani and Anne Roudaut. 2017. Frozen Suit: Designing a Changeable Stiffness Suit and its Application to Haptic Games. In *Proceedings of the 2017 CHI Conference on Human Factors in Computing Systems* (Denver, Colorado, USA) (CHI '17). Association for Computing Machinery, New York, NY, USA, 2440–2448. <https://doi.org/10.1145/3025453.3025655>
- [2] Lea Albaugh, Scott Hudson, and Lining Yao. 2019. Digital Fabrication of Soft Actuated Objects by Machine Knitting. In *Proceedings of the 2019 CHI Conference on Human Factors in Computing Systems* (Glasgow, Scotland UK) (CHI '19). Association for Computing Machinery, New York, NY, USA, 1–13. <https://doi.org/10.1145/3290605.3300414>
- [3] Bernd Bickel, Moritz Bäcker, Miguel A. Otaduy, Hyunho Richard Lee, Hanspeter Pfister, Markus Gross, and Wojciech Matusik. 2010. Design and fabrication of materials with desired deformation behavior. *ACM Trans. Graph.* 29, 4, Article 63 (jul 2010), 10 pages. <https://doi.org/10.1145/1778765.1778800>
- [4] Tian Chen, Mark Pauly, and Pedro M Reis. 2021. A reprogrammable mechanical metamaterial with stable memory. *Nature* 589, 7842 (2021), 386–390.
- [5] Inrak Choi, Heather Culbertson, Mark R. Miller, Alex Olwal, and Sean Follmer. 2017. Grability: A Wearable Haptic Interface for Simulating Weight and Grasping in Virtual Reality. In *Proceedings of the 30th Annual ACM Symposium on User Interface Software and Technology* (Québec City, QC, Canada) (UIST '17). Association for Computing Machinery, New York, NY, USA, 119–130. <https://doi.org/10.1145/3126594.3126599>
- [6] Inrak Choi and Sean Follmer. 2016. Wolverine: A Wearable Haptic Interface for Grasping in VR. In *Adjunct Proceedings of the 29th Annual ACM Symposium on User Interface Software and Technology* (Tokyo, Japan) (UIST '16 Adjunct). Association for Computing Machinery, New York, NY, USA, 117–119. <https://doi.org/10.1145/2984751.2985725>
- [7] Himani Deshpande, Bo Han, Kongpyung Moon, Andrea Bianchi, Clement Zheng, and Jeeun Kim. 2024. Reconfigurable Interfaces by Shape Change and Embedded Magnets. In *Proceedings of the CHI Conference on Human Factors in Computing Systems*. 1–12.
- [8] Cathy Fang, Yang Zhang, Matthew Dworman, and Chris Harrison. 2020. Wireality: Enabling Complex Tangible Geometries in Virtual Reality with Worn Multi-String Haptics. In *Proceedings of the 2020 CHI Conference on Human Factors in Computing Systems* (<conf-loc>, <city>Honolulu</city>, <state>HI</state>, <country>USA</country>, </conf-loc>) (CHI '20). Association for Computing Machinery, New York, NY, USA, 1–10. <https://doi.org/10.1145/3313831.3376470>
- [9] Sean Follmer, Daniel Leithinger, Alex Olwal, Akimitsu Hogge, and Hiroshi Ishii. 2013. inFORM: dynamic physical affordances and constraints through shape and object actuation. In *Proceedings of the 26th Annual ACM Symposium on User Interface Software and Technology* (St. Andrews, Scotland, United Kingdom) (UIST '13). Association for Computing Machinery, New York, NY, USA, 417–426. <https://doi.org/10.1145/2501988.2502032>
- [10] Benjamin M Goldsberry and Michael R Haberman. 2018. Negative stiffness honeycombs as tunable elastic metamaterials. *Journal of applied physics* 123, 9 (2018).
- [11] Jesse T Gonzalez, Sonia Prashant, Sapna Tayal, Juhi Kedia, Alexandra Ion, and Scott E Hudson. 2023. Constraint-Driven Robotic Surfaces, At Human-Scale. In *Proceedings of the 36th Annual ACM Symposium on User Interface Software and Technology* (San Francisco, CA, USA) (UIST '23). Association for Computing Machinery, New York, NY, USA, Article 53, 12 pages. <https://doi.org/10.1145/3586183.3606740>
- [12] Daniel Groeger, Elena Chong Loo, and Jürgen Steimle. 2016. HotFlex: Post-print Customization of 3D Prints Using Embedded State Change. In *Proceedings of the 2016 CHI Conference on Human Factors in Computing Systems* (San Jose, California, USA) (CHI '16). Association for Computing Machinery, New York, NY, USA, 420–432. <https://doi.org/10.1145/2858036.2858191>

- [13] Violet Yinuo Han, Abena Boadi-Agyemang, Yuyu Lin, David Lindlbauer, and Alexandra Ion. 2023. Parametric Haptics: Versatile Geometry-based Tactile Feedback Devices. In *Proceedings of the 36th Annual ACM Symposium on User Interface Software and Technology* (<conf-loc>, <city>San Francisco</city>, <state>CA</state>, <country>USA</country>, </conf-loc>) (UIST '23). Association for Computing Machinery, New York, NY, USA, Article 65, 13 pages. <https://doi.org/10.1145/3586183.3606766>
- [14] Takeru Hashimoto, Shigeo Yoshida, and Takuji Narumi. 2022. MetamorphX: An Ungrounded 3-DoF Moment Display that Changes its Physical Properties through Rotational Impedance Control. In *Proceedings of the 35th Annual ACM Symposium on User Interface Software and Technology* (Bend, OR, USA) (UIST '22). Association for Computing Machinery, New York, NY, USA, Article 72, 14 pages. <https://doi.org/10.1145/3526113.3545650>
- [15] Alexandra Ion, Johannes Frohnhofen, Ludwig Wall, Robert Kovacs, Mirela Alistar, Jack Lindsay, Pedro Lopes, Hsiang-Ting Chen, and Patrick Baudisch. 2016. Metamaterial Mechanisms. In *Proceedings of the 29th Annual Symposium on User Interface Software and Technology* (Tokyo, Japan) (UIST '16). Association for Computing Machinery, New York, NY, USA, 529–539. <https://doi.org/10.1145/2984511.2984540>
- [16] Alexandra Ion, Robert Kovacs, Oliver S. Schneider, Pedro Lopes, and Patrick Baudisch. 2018. Metamaterial Textures. In *Proceedings of the 2018 CHI Conference on Human Factors in Computing Systems* (Montreal QC, Canada) (CHI '18). Association for Computing Machinery, New York, NY, USA, 1–12. <https://doi.org/10.1145/3173574.3173910>
- [17] Alexandra Ion, Ludwig Wall, Robert Kovacs, and Patrick Baudisch. 2017. Digital Mechanical Metamaterials. In *Proceedings of the 2017 CHI Conference on Human Factors in Computing Systems* (Denver, Colorado, USA) (CHI '17). Association for Computing Machinery, New York, NY, USA, 977–988. <https://doi.org/10.1145/3025453.3025624>
- [18] Seungwoo Je, Hyunseung Lim, Kongpyung Moon, Shan-Yuan Teng, Jas Brooks, Pedro Lopes, and Andrea Bianchi. 2021. Elevate: A Walkable Pin-Array for Large Shape-Changing Terrains. In *Proceedings of the 2021 CHI Conference on Human Factors in Computing Systems* (Yokohama, Japan) (CHI '21). Association for Computing Machinery, New York, NY, USA, Article 127, 11 pages. <https://doi.org/10.1145/3411764.3445454>
- [19] Yu Jiang, Shobhit Aggarwal, Zhipeng Li, Yuanchun Shi, and Alexandra Ion. 2023. Reprogrammable Digital Metamaterials for Interactive Devices. In *Proceedings of the 36th Annual ACM Symposium on User Interface Software and Technology* (<conf-loc>, <city>San Francisco</city>, <state>CA</state>, <country>USA</country>, </conf-loc>) (UIST '23). Association for Computing Machinery, New York, NY, USA, Article 56, 15 pages. <https://doi.org/10.1145/3586183.3606752>
- [20] Mirela Kahrmanovic, Wouter M Bergmann Tiest, and Astrid ML Kappers. 2011. Discrimination thresholds for haptic perception of volume, surface area, and weight. *Attention, perception, & psychophysics* 73 (2011), 2649–2656.
- [21] Ozgun Kilic Afsar, Ali Shtarbanov, Hila Mor, Ken Nakagaki, Jack Forman, Karen Modrei, Seung Hee Jeong, Klas Hjort, Kristina Höök, and Hiroshi Ishii. 2021. OmniFiber: Integrated Fluidic Fiber Actuators for Weaving Movement based Interactions into the 'Fabric of Everyday Life'. In *The 34th Annual ACM Symposium on User Interface Software and Technology* (Virtual Event, USA) (UIST '21). Association for Computing Machinery, New York, NY, USA, 1010–1026. <https://doi.org/10.1145/3472749.3474802>
- [22] Hyunyoung Kim, Céline Coutrix, and Anne Roudaut. 2018. KnobSlider: Design of a Shape-Changing UI for Parameter Control. In *Proceedings of the 2018 CHI Conference on Human Factors in Computing Systems* (<conf-loc>, <city>Montreal QC</city>, <country>Canada</country>, </conf-loc>) (CHI '18). Association for Computing Machinery, New York, NY, USA, 1–13. <https://doi.org/10.1145/3173574.3173913>
- [23] Hyunyoung Kim, Patrícia Deud Guimarães, Céline Coutrix, and Anne Roudaut. 2019. ExpanDial: Designing a Shape-Changing Dial. In *Proceedings of the 2019 Designing Interactive Systems Conference* (San Diego, CA, USA) (DIS '19). Association for Computing Machinery, New York, NY, USA, 949–961. <https://doi.org/10.1145/3322276.3322283>
- [24] Kuan Liang, Yaguang Wang, Yangjun Luo, Akihiro Takezawa, Xiaopeng Zhang, and Zhan Kang. 2023. Programmable and multistable metamaterials made of precisely tailored bistable cells. *Materials & Design* 227 (2023), 111810. <https://doi.org/10.1016/j.matdes.2023.111810>
- [25] Yuyu Lin, Jesse T Gonzalez, Zhitong Cui, Yash Rajeev Banka, and Alexandra Ion. 2024. ConeAct: A Multistable Actuator for Dynamic Materials. In *Proceedings of the CHI Conference on Human Factors in Computing Systems* (Honolulu, HI, USA) (CHI '24). Association for Computing Machinery, New York, NY, USA, Article 324, 16 pages. <https://doi.org/10.1145/3613904.3642949>
- [26] Pedro Lopes, Patrik Jonell, and Patrick Baudisch. 2015. Affordance++: Allowing Objects to Communicate Dynamic Use. In *Proceedings of the 33rd Annual ACM Conference on Human Factors in Computing Systems* (Seoul, Republic of Korea) (CHI '15). Association for Computing Machinery, New York, NY, USA, 2515–2524. <https://doi.org/10.1145/2702123.2702128>
- [27] Pedro Lopes, Sijing You, Lung-Pan Cheng, Sebastian Marwecki, and Patrick Baudisch. 2017. Providing Haptics to Walls & Heavy Objects in Virtual Reality by Means of Electrical Muscle Stimulation. In *Proceedings of the 2017 CHI Conference on Human Factors in Computing Systems* (Denver, Colorado, USA) (CHI '17). Association for Computing Machinery, New York, NY, USA, 1471–1482. <https://doi.org/10.1145/3025453.3025600>
- [28] Jasmine Lu, Ziwei Liu, Jas Brooks, and Pedro Lopes. 2021. Chemical Haptics: Rendering Haptic Sensations via Topical Stimulants. In *The 34th Annual ACM Symposium on User Interface Software and Technology* (Virtual Event, USA) (UIST '21). Association for Computing Machinery, New York, NY, USA, 239–257. <https://doi.org/10.1145/3472749.3474747>
- [29] Qiuyu Lu, Haiqing Xu, Yijie Guo, Joey Yu Wang, and Lining Yao. 2023. Fluidic Computation Kit: Towards Electronic-free Shape-changing Interfaces. In *Proceedings of the 2023 CHI Conference on Human Factors in Computing Systems* (>Hamburg, Germany) (CHI '23). Association for Computing Machinery, New York, NY, USA, Article 211, 21 pages. <https://doi.org/10.1145/3544548.3580783>
- [30] Anders Lundström and Ylva Fernaeus. 2022. Making Crank-Powered Interactions: Methods, Demonstrators, Materials. In *Proceedings of the 2022 ACM Designing Interactive Systems Conference* (Virtual Event, Australia) (DIS '22). Association for Computing Machinery, New York, NY, USA, 913–924. <https://doi.org/10.1145/3532106.3533453>
- [31] Jasmine C Menant, Julie R Steele, Hylton B Menz, Bridget J Munro, and Stephen R Lord. 2009. Effects of walking surfaces and footwear on tempo-spatial gait parameters in young and older people. *Gait & posture* 29, 3 (2009), 392–397.
- [32] Sachith Muthukumarana, Moritz Alexander Messerschmidt, Denys J.C. Matthies, Jürgen Steimle, Philipp M. Scholl, and Suranga Nanayakkara. 2021. ClothTiles: A Prototyping Platform to Fabricate Customized Actuators on Clothing using 3D Printing and Shape-Memory Alloys. In *Proceedings of the 2021 CHI Conference on Human Factors in Computing Systems* (Yokohama, Japan) (CHI '21). Association for Computing Machinery, New York, NY, USA, Article 510, 12 pages. <https://doi.org/10.1145/3411764.3445613>
- [33] Ken Nakagaki, Sean Follmer, and Hiroshi Ishii. 2015. LineFORM: Actuated Curve Interfaces for Display, Interaction, and Constraint. In *Proceedings of the 28th Annual ACM Symposium on User Interface Software and Technology* (Charlotte, NC, USA) (UIST '15). Association for Computing Machinery, New York, NY, USA, 333–339. <https://doi.org/10.1145/2807442.2807452>
- [34] Ken Nakagaki, Luke Vink, Jared Counts, Daniel Windham, Daniel Leithinger, Sean Follmer, and Hiroshi Ishii. 2016. Materible: Rendering Dynamic Material Properties in Response to Direct Physical Touch with Shape Changing Interfaces. In *Proceedings of the 2016 CHI Conference on Human Factors in Computing Systems* (San Jose, California, USA) (CHI '16). Association for Computing Machinery, New York, NY, USA, 2764–2772. <https://doi.org/10.1145/2858036.2858104>
- [35] Jifei Ou, Zhao Ma, Jannik Peters, Sen Dai, Nikolaos Vlavianos, and Hiroshi Ishii. 2018. KinetiX-designing auxetic-inspired deformable material structures. *Computers & Graphics* 75 (2018), 72–81.
- [36] Julian Panetta, Qingnan Zhou, Luigi Malomo, Nico Pietroni, Paolo Cignoni, and Denis Zorin. 2015. Elastic textures for additive fabrication. *ACM Trans. Graph.* 34, 4, Article 135 (jul 2015), 12 pages. <https://doi.org/10.1145/2766937>
- [37] Fang Qin, Huai-Yu Cheng, Rachel Sneeringer, Maria Vlachostergiou, Sampada Acharya, Haolin Liu, Carmel Majidi, Mohammad Islam, and Lining Yao. 2021. ExoForm: Shape Memory and Self-Fusing Semi-Rigid Wearables. In *Extended Abstracts of the 2021 CHI Conference on Human Factors in Computing Systems* (Yokohama, Japan) (CHI EA '21). Association for Computing Machinery, New York, NY, USA, Article 249, 8 pages. <https://doi.org/10.1145/3411763.3451818>
- [38] Mark S Redfern and Bopaya Bidanda. 1994. Slip resistance of the shoe-floor interface under biomechanically-relevant conditions. *Ergonomics* 37, 3 (1994), 511–524.
- [39] Krishna Kumar Saxena, Raj Das, and Emilio P Calius. 2016. Three decades of auxetics research- materials with negative Poisson's ratio: a review. *Advanced Engineering Materials* 18, 11 (2016), 1847–1870.
- [40] Giulia Scalet. 2024. Programmable materials: Current trends, challenges, and perspectives. *Applied Materials Today* 40 (2024), 102372. <https://doi.org/10.1016/j.apmt.2024.102372>
- [41] Christian Schumacher, Bernd Bickel, Jan Rys, Steve Marschner, Chiara Daraio, and Markus Gross. 2015. Microstructures to control elasticity in 3D printing. *ACM Trans. Graph.* 34, 4, Article 136 (jul 2015), 13 pages. <https://doi.org/10.1145/2766926>
- [42] Sicong Shan, Sung H Kang, Jordan R Raney, Pai Wang, Lichen Fang, Francisco Candido, Jennifer A Lewis, and Katia Bertoldi. 2015. Multistable architected materials for trapping elastic strain energy. *Adv. Mater* 27, 29 (2015), 4296–4301.
- [43] Jotaro Shigeyama, Takeru Hashimoto, Shigeo Yoshida, Takuji Narumi, Tomohiro Tanikawa, and Michitaka Hirose. 2019. Transcalibur: A Weight Shifting Virtual Reality Controller for 2D Shape Rendering based on Computational Perception Model. In *Proceedings of the 2019 CHI Conference on Human Factors in Computing Systems* (Glasgow, Scotland UK) (CHI '19). Association for Computing Machinery, New York, NY, USA, 1–11. <https://doi.org/10.1145/3290605.3300241>
- [44] Ryo Suzuki, Ryosuke Nakayama, Dan Liu, Yasuaki Kakehi, Mark D. Gross, and Daniel Leithinger. 2020. LiftTiles: Constructive Building Blocks for Prototyping Room-scale Shape-changing Interfaces. In *Proceedings of the Fourteenth International Conference on Tangible, Embedded, and Embodied Interaction* (Sydney NSW,

- Australia) (*TEI '20*). Association for Computing Machinery, New York, NY, USA, 143–151. <https://doi.org/10.1145/3374920.3374941>
- [45] Yujie Tao, Shan-Yuan Teng, and Pedro Lopes. 2021. Altering Perceived Softness of Real Rigid Objects by Restricting Fingerpad Deformation. In *The 34th Annual ACM Symposium on User Interface Software and Technology* (Virtual Event, USA) (*UIST '21*). Association for Computing Machinery, New York, NY, USA, 985–996. <https://doi.org/10.1145/3472749.3474800>
- [46] Shan-Yuan Teng, K. D. Wu, Jacqueline Chen, and Pedro Lopes. 2022. Prolonging VR Haptic Experiences by Harvesting Kinetic Energy from the User. In *Proceedings of the 35th Annual ACM Symposium on User Interface Software and Technology* (Bend, OR, USA) (*UIST '22*). Association for Computing Machinery, New York, NY, USA, Article 39, 18 pages. <https://doi.org/10.1145/3526113.3545635>
- [47] Guanyun Wang, Humphrey Yang, Zeyu Yan, Nurcan Gecer Ulu, Ye Tao, Jianzhe Gu, Levent Burak Kara, and Lining Yao. 2018. 4D Mesh: 4D Printing Morphing Non-Developable Mesh Surfaces. In *Proceedings of the 31st Annual ACM Symposium on User Interface Software and Technology* (Berlin, Germany) (*UIST '18*). Association for Computing Machinery, New York, NY, USA, 623–635. <https://doi.org/10.1145/3242587.3242625>
- [48] Willa Yunqi Yang, Yumeng Zhuang, Luke Darcy, Grace Liu, and Alexandra Ion. 2022. Reconfigurable Elastic Metamaterials. In *Proceedings of the Annual ACM Symposium on User Interface Software and Technology* (Bend, Oregon, USA) (*UIST '22*). Association for Computing Machinery, New York, NY, USA. <https://doi.org/10.1145/3526113.3545649>
- [49] Lining Yao, Jifei Ou, Chin-Yi Cheng, Helene Steiner, Wen Wang, Guanyun Wang, and Hiroshi Ishii. 2015. bioLogic: Natto Cells as Nanoactuators for Shape Changing Interfaces. In *Proceedings of the 33rd Annual ACM Conference on Human Factors in Computing Systems* (Seoul, Republic of Korea) (*CHI '15*). Association for Computing Machinery, New York, NY, USA, 1–10. <https://doi.org/10.1145/2702123.2702611>
- [50] Clement Zheng, Zhen Zhou Yong, Hongnan Lin, HyunJoo Oh, and Ching Chiuang Yen. 2022. Shape-haptics: planar & passive force feedback mechanisms for physical interfaces. In *Proceedings of the 2022 CHI Conference on Human Factors in Computing Systems*. 1–15.
- [51] Shannon A. Zirbel, Kyler A. Tolman, Brian P. Trease, and Larry L. Howell. 2016. Bistable Mechanisms for Space Applications. *PLOS ONE* 11, 12 (12 2016), 1–18. <https://doi.org/10.1371/journal.pone.0168218>